Silicon (2020) 12:2211–2220
https://doi.org/10.1007/s12633-019-00309-z

ORIGINAL PAPER

Experimental Investigation of Wire-Electrochemical Discharge Machining (WECDM) Performance Characteristics for Quartz Material

Manoj Kumar[1] · Rahul O. Vaishya[1] · Ankit D. Oza[2] · Narendra M. Suri[1]

Received: 4 June 2019 / Accepted: 25 October 2019 / Published online: 28 November 2019

Abstract

The machining of quartz due to hard, non-conducting and brittle behavior with desired accuracy and precision is always a challenge. Quartz is widely used in MEMS/MOEMS applications. However, wire electrochemical discharge machining (WECDM) has great potential to machine hard and brittle materials like quartz, glass FRP, etc. The WECDM process is a hybrid non-conventional manufacturing process which combines characteristics of electrochemical machining (ECM) and wire-electrical discharge machining (W-EDM). The present study discusses the investigation of the effect of the governing process parameters such as voltage, electrolyte concentration, and wire speed (feed) on material removal rate (MRR) and surface roughness (Ra) during the micro-machining of quartz using self-developed tabletop desktop WECDM setup. The hybrid methodology of Taguchi orthogonal arrays and Analysis of variance (ANOVA) is used to find the optimum parameters and their significant contribution to response parameters respectively. Experimental results reveal that a better surface finish and high material removal rate was obtained by zinc layered brass wire (150 μm diameter). The machining of quartz under the zinc layered brass wire can indeed enhance the surface quality characteristics and material removal rate. Also, the mathematical models were established in order to derive the relationship between input and response parameters which was successfully validated by the confirmation experiment. Furthermore, the machining quality observed by a Scanning electron microscope (SEM), reveals the presence shallow cracks at higher-end input parameters.

Keywords WECDM · Micro-machining · Quartz · Layered wire · MRR · R_a

Nomenclature

ECDM	Electro-chemical discharge machining
WECDM	Wire electro-chemical discharge machining
MOEMS	Micro-optical electromechanical system
FRP	Fiber-reinforced plastic
MEMS	Micro electro mechanical system
LBM	Laser beam machining
USM	Ultrasonic machining
W-EDM	Wire-electro discharge machining
ECM	Electrochemical machining
DC	Direct current
AC	Alternative current
MRR	Material removal rate
MSD	Mean square deviation
S/N	ratio Signal to noise ratio
V	Voltage
OA	Orthogonal array
ANOVA	Analysis of variance
SEM	Scanning electron microscope
K_w	Kerf width
R_a	Surface roughness
%	Percentage
DOF	Degrees of freedom

✉ Manoj Kumar
mnjbrd.02@gmail.com

Rahul O. Vaishya
rahul_mv@yahoo.com

Ankit D. Oza
ankit.ophd15@sot.pdpu.ac.in

Narendra M. Suri
nmsuri65@yahoo.com

[1] Punjab Engineering College, Deemed to be University, Chandigarh 160012, India

[2] Pandit Deendayal Petroleum University, Gandhinagar 382007, India

1 Introduction

Glass and its variants (soda-lime, borosilicate, pyrex glass, etc.) are used in the daily use applications such as mirrors, bottles, vehicle/window glasses to advance scientific applications such as telescope lenses, fibre optics, radiation protectors, etc. Glass material is widely used in the Micro-Electro-Mechanical System (MEMS)/Micro-Optical-Electro-Mechanical System (MOEMS) which are used as sensors in electronics, aerospace, life science, optics, imaging, lighting, and home appliance. Quartz glass is a pure form of silica having SiO_2 content more than 99.9%. Due to this, it possesses better working properties such as high hardness, corrosion resistance, stability under atomic bombardment and better optical transmission over other glass materials. It can work at higher temperature, therefor can be used in the optical fiber, EPROM (erasable programmable read-only memory), benthoscope, special lenses such as in telescope, Nikon and various optical measuring devices. Due to these qualities machining characteristics and performance of quartz glass is needed to study [1].

Quartz has high hardness, this makes quartz glass difficult to machine by conventional machining process as it leads to higher cutting forces that result in brittle fracture. However, the quartz glass can be machined by a single-point cutting tool in ductile regime with good surface roughness and crack-free surface [2] but the high cost of diamond tool and wear limits the use of the process. The non-conventional machining process such as ultrasonic machining can machine the quartz glass but the tool wear and effectiveness of abrasive powder deteriorates after a certain duration of machining time [3]. The kerf width (taper) [4], complexity and environment issues are the main barriers of abrasive water jet machining (AWJM) process. The laser machining of quartz glass is possible [5] but energy consumption and cost are very high. Being a non-conducting material, other advance machining processes such as wire or electric discharge machining (W-EDM or EDM) and electric chemical machining (ECM) cannot machine quartz material directly.

Wire electrochemical discharge machining (WECDM) process, a variant of electrochemical discharge machining (ECDM) which is a further hybrid process of ECM and WEDM, can cut non-conducting materials. WECDM has established itself as a cost-effective alternative solution to earlier existing processes such as USM, AWJM and laser machining. The process was developed in 1985, so the process is still limited to research and has not commercialized due to few limitations. Consistent research has been going on to develop the process. Therefore, this study is an attempt to explore the possibilities and difficulties arisen during the micro-slicing of quartz glass using developed WECDM setup. Some past research data has been found which is discussed as follows.

Jain et al. [6] machined the composites (kevlar epoxy and glass epoxy) using traveling wire electrochemical discharge machining TW-ECDM process. Material removal rate (MRR) was increased by supplying the bubble externally around the cathode. To improve the performance of the process, Oza et al. [7] investigated the characteristics like Material removal rate and kerf width for traveling wire electrochemical discharge machining process using zinc-coated brass wire of 0.15 mm diameter and concluded that voltage and electrolyte concentration are main significant parameters of the process. Yang et al. [8] used the pulsed DC voltage and weight loading mechanism for feeding of the workpiece with the SiC abrasive in the electrolyte and found that the surface roughness improves with the addition of abrasives. Kuo et al. [9] suggested that the surface roughness (SR) and average slit deviation can be improved by adding SiC abrasives to the electrolyte. However, SiC abrasive disturbs the gas film formation. Bhuyan and Yadava [10] studied the WECDM process by conducting the experiments using Taguchi method gray relation analysis (TMGRA) for optimization, The improvement in the response parameters surface roughness and material removal rate was found to be 10% and 117% respectively. Rattan and Mulik [11] conducted the experiments by applying the magnetic field in WECDM using the permanent magnet. After using the regression model, the optimal value obtained for material removal rate and surface roughness was 0.50 mg/min and 9.60 μm respectively. Rattan and Mulik [12] improved the electrolyte circulation by enriching the magnetohydrodynamic (MHD) convection. The material removal rate increases from 9.09% to 200% under different experimental conditions. Bhuyan and Yadava [13] performed the experimentation using the borosilicate glass for material removal rate and kerf width. Microscopic images were taken, suggest that at high voltage and low wire tension. There is problem of unusual irregular shape of the heat-affected zone (HAZ) at the bottom side kerf width along with tiny crater sand shallow cracks due to high electrolyte concentration. Bhuyan and Yadava [14] developed the mathematical model for WECDM process during the experimentation of pyrex glass and claimed that there is an improvement in material removal rate, surface roughness and kerf width is obtained by 154%, 21%, and 11% respectively. Peng et al. [15] performed different experiments to find suitable parameters for machining of optical glass and quartz bars. It was reported that pulsed DC power supply has better spark stability than regular DC power supply. Mitra et al. [16] predicted the response parameters using an artificial neural network (feed forward back propagation) for machining the hylam composite. The error prediction for material removal rate was high compared to radial overcut (ROC). Table 1 shows the summary of literature survey in WECDM process.

Table 1 Summary of WECDM literature

Authors	Tool (Wire)	Workpiece material	Electrolyte	Auxiliary Electrode	Input parameters	Response parameters	DOE	Conclusion/Finding/Inference/Contribution
Mitra et al. [16]	Brass wire Φ0.25 mm	Hylam composite, 3 mm thickness	KOH	–	Pulse on time Frequency Electrolyte Concentration Wire feed Voltage	MRR ROC	Taguchi L25 orthogonal array (OA) Empirical model RSM ANN prediction (feed forward back propagation neural network)	First-time Neural network was proposed to predict the response parameters, which were further optimized by Taguchi based optimization along with regression analysis.
Malik and Manna [17]	Brass wire Φ0.2 mm	E-glass fibre epoxy composite	NaOH	Copper	Voltage Concentration Wire speed IE gap Current	MRR Spark gap width	Taguchi 4^5 OA	Voltage and electrolyte concentration contribute more than 95% for the material removal rate. Along with machined surface, slight uncut fibers were observed, might be due to the non-circulation of electrolyte at machining zone.
Bhuyan and Yadava [13]	Brass wire Φ0.25 mm	Borosilicate glass 40 × 35 × 2 mm	NaOH	Graphite Φ8 mm L-55 mm	Voltage Pulse on pulse off electrolyte concentration	MRR Kerf width	Effect of input parameters (3 levels) by varying the wire feed for both response parameters	Due to high concentration, shallow cracks were formed across the machined surface and due to the high melting point of borosilicate glass, the surface cut was not smooth.
Liu et al. [18]	Molybdenum wire Φ0.18 mm	Al_2O_3 (10% & 20%) Alloy/composite Rolled plate 36 mm	Water-based emulsion ($NaNO_3$ added to enhance conductivity)	–	Voltage Pulse on current	MRR 10% 20%	L9 3^4 OA	The emulsion electrolyte promotes the ECM action at the high concentration by increasing the current density with a decrease in EDM action.
Peng & Liao [15]	Copper and Stainless wire Φ0.25 mm	Optical and quartz bar	KOH NaOH	–	Frequency and duty factor Voltage Electrolyte Reactive wire length	1.Spark stability 2.paraemters combinations for slicing	–	The spark characteristic across the machining zone has better performance for KOH electrolyte over NaOH & DC power supply over continuous power supply, improves the process efficiency. Glass has better machining surface compared to quartz in terms of transparency and surface finish.
Pallvita et al. [19]	Brass wire Φ0.2 mm	Alumina epoxy composite, T-3 mm	NaOH	Graphite	Voltage Concentration Pulse on time Pulse off time	Kerf thickness Kerf deviations	By varying the feed, at 3 levels output parameters were studied	Kerf deviation increases with increase in the voltage & pulse on time and decreases with a decrease in pulse off time.
Oza et al. [7]	Zn coated wire Φ0.15 mm	Quartz glass 75 × 25 × 2 mm	NaOH	Graphite Φ20 mm, L-80 mm	Voltage Concentration Wire speed	MRR Kerf width	L9 orthogonal array	The fine coated wire improves the machining performance due to better spark stability.
Bhuyan and Yadava [14]	Brass wire Φ0.25 mm	Pyrex glass 40 × 35 × 2 mm	NaOH	Graphite Φ8 mm, L-55 mm	Voltage Pulse on time Pulse off time Concentration Wire feed	MRR SR K_W	L27 OA TMRSM GRAPCA	The process is significantly improved after optimization technique for response parameters MRR, SR, and Kerf width by 154%, 21%, and 11% respectively
Kuo et al. [20]	CuZn73 brass wire	Quartz glass 5 × 7 × 1 mm	KOH 5 M	Graphite electrode 16 × 16 × 5 mm	Electrolyte droplet Voltage	Machining depth	–	A cost-effective and less polluted way of electrolyte circulation was proposed by titrated electrolyte flow which

Table 1 (continued)

Authors	Tool (Wire)	Workpiece material	Electrolyte	Auxiliary Electrode	Input parameters	Response parameters	DOE	Conclusion/Finding/Inference/Contribution
					Electrolyte flow rate Electrolyte flow mode			improved the machining performance and surface integrity.
Yang et al. [8]	Brass wire Φ0.25 mm	Pyrex glass	KOH NaOH	Graphite plate	Abrasive concentration and grit size Power frequency and duty factor Electrolyte Wire tension wire feed rate	At different electrolyte concentration, with 4 levels of each input parameters studied by the graph	–	The process was improved by SiC abrasive particles, which improves the surface quality and lower the formation of microcracks.

1.1 Principle & Mechanism of Material Removal Rate

In the WECDM process, the material is removed by the thermal spark as well as the chemical action of electrolyte. The spark is generated between tool wire (cathode) and electrolyte. When there is sufficient potential difference between cathode and anode (auxiliary electrode), this thermal spark generates a high temperature. As the workpiece (quartz) is kept in the vicinity of thermal spark, melting and vaporization of workpiece take place.

Basak and Ghosh [21] proposed the theoretical model to explain the discharge by modeling the process as switching phenomena in an electrical circuit. As the DC voltage increases beyond the critical voltage, under the action of electrochemical reaction, the hydrogen gas evolves at cathode and oxygen at anode, which leads to bubble formation. The bubbles grow in size with time and coalescence to bigger ones, which shield the cathode in the electrolyte. Due to the constriction effect, the resistance across the tool and electrode interface increases. The induced emf (E) is given by Eq. 1.

$$E = -L\frac{dI}{dt} \tag{1}$$

Where I is the instantaneous current, L is the inductance of the circuit.

This leads to breaking the current supply for a short time that is analogues to switching off mechanism. Later, Basak and Ghosh [22] mathematically derived the equation for the material removal rate. The theoretical results were closely matched with experimental results. McGeough et al. [23] studied the single pulse discharge with the help of high-speed imaging and oscilloscope and reported the four different stages namely high-frequency oscillation, high rate ECM, low rate ECM and EDM action in which discharge proceeds. Jain et al. [24] proposed valve theory to explain the discharge mechanism by neglecting the inductive effect. When the gas pressure is different at inside as well as outside the tube, then breakdown results in electric discharge under high potential gradient.

2 Experimental Methodology

2.1 Experimental Setup

WECDM setup is fabricated in-house to study the process experimentally and to evaluate the effect of governing parameters on machining performance. Figure 1 shows the schematic diagram of the setup consisting of machine structure (body), power supply, motion controller system and other components such as tool wire, electrolyte, auxiliary electrode.

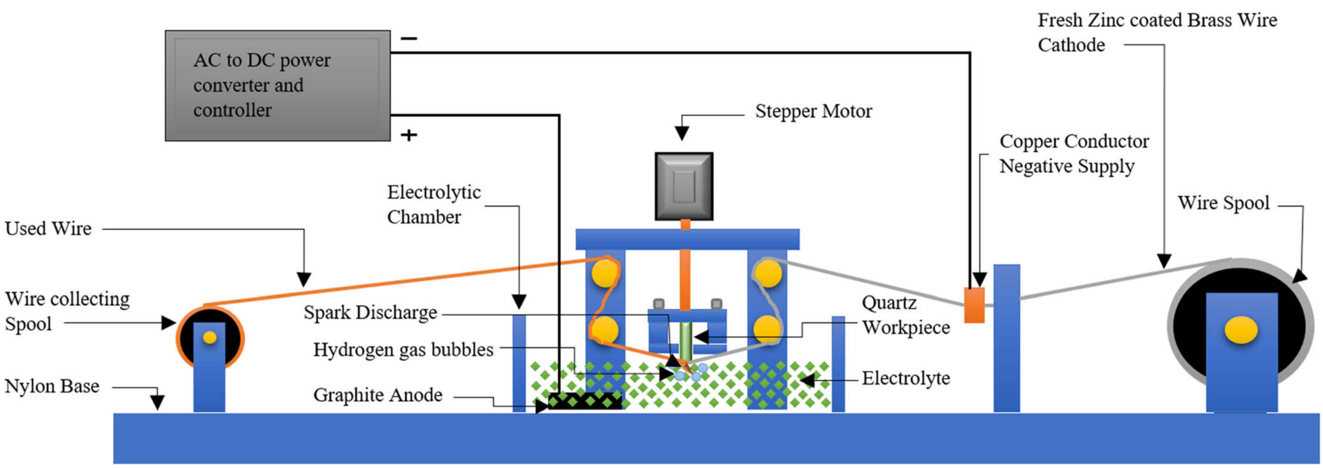

Fig. 1 Experimental setup for WECDM setup [1]

The outer structure was made up of a nylon sheet of 20 mm thickness which consists of four pulleys to provide proper tension to tool wire. A small hollow cylindrical rod was attached to it at the right mid-end of the setup to provide the conductivity to wire. The workpiece fixture of the same material was fabricated, the motion of which was regulated by a lead screw mechanism. The machining electrolyte tank of 18 × 100 × 50 mm dimensions were made up of insulating and non-corrosive acrylic sheet. One sidewall of the tank was calibrated to check the electrolyte level, further, at the bottom side, a small tap was also enclosed for cleaning and discharging purposes.

The motion system of the setup consists of the stepper motor which is used to feed the wire spool, which was further controlled by micro-stepping drivers through the electronic circuit board. The CNC MACH3 software package was used to precisely control the motions. The switch-mode power system (SMPS) was used which provides the power requirements of the stepper motors.

To convert the 230 V AC normal household power supply to usable DC power, a separate DC power system consisting of a step-down transformer, rectifier, and other subcomponents was used having a voltage output of 0–120 V and current 0–10 A range. The DC power system was used to avoid the cycling effect of AC across both the electrodes. The output terminals i.e. positive and negative points of DC power system were connected to the auxiliary electrode (anode) and the tool wire (cathode) respectively for straight polarity. A small rating UPS was also employed for the backup of 25 minutes duration. The rectangular quartz material and zinc layered brass wire were used as workpiece and tool wire respectively. The detailed specifications of the workpiece (quartz) and tool wire are shown in Tables 2 and 3.

2.2 Experimental Plan

In the present research work, material removal rate and surface roughness are studied for machining the quartz by Taguchi design of experiment. Based on the initial trial experiments, the levels of the input parameters were selected. Table 4 shows the input process parameters and their levels. The input voltage, electrolyte concentration, and wire speed (feed) were considered as input parameters. Taguchi orthogonal (L_9) design was used to analyze the parameters. In the Taguchi design, Signal to Noise (S/N) ratio is used to find the optimum parameters for machining both the response parameters. Also, the S/N ratio is used to measure the quality characteristics deviating from the desired value. Table 5 shows the S/N ratio for response parameters as per Taguchi L9 orthogonal array. The ANOVA was used to find the relative contribution of each input machining parameters on the response parameters. Tables 6 and 7 shows ANOVA tables for Material removal rate and surface roughness. The contribution (%) of each input

Table 2 Quartz material specifications

Dimensions	75 × 25 × 1 mm
Silica content	>99.995%
Density	2.2×10^3 Kg/m^3
Hardness (Mohr's scale)	6
Melting point	1650 °C
Tensile strength	70 N/mm^2

Table 3 Tool wire specification

Material	Zn layered brass wire (grade- hard)
Diameter	0.15 mm
Diameter tolerance	+0.00/−0.002 mm
Tensile strength	900 N/mm^2
Elongation	3%
Conductivity	12–14%

Table 4 Process parameters and levels

Factors	levels		
	1	2	3
Voltage (A) (volt)	36	41	46
Electrolyte concentration (B) (%) (g/L)	35	40	45
Wire speed (C) (m/min)	2	7	12

parameter on the material removal rate (MRR) and surface roughness (R_a) is evaluated by Eq. 2. Where SS_d and SS_T are the sums of squared deviation and total sum of squared deviation respectively.

$$\text{Contribution}\ (\%) = \left(\frac{SS_d}{SS_T}\right) \tag{2}$$

Material removal is evaluated as a change in the weight of the workpiece during the machining. The Material removal rate (MRR) is calculated by means of Eq. 3. The Weight of the workpiece is measured by Denver SI 234 having a digital balance with an accuracy of 0.01 mg. The surface roughness (R_a) is determined by Mitutoyo SJ-400. The mean of the two readings was taken as the final reading for evaluation.

$$MRR = \frac{\left(M_b - M_a\right)}{t} \tag{3}$$

Where,

M_b weight of workpiece before the investigation (mg)
M_a weight of workpiece after the investigation (mg)
t machining time during micro-slicing (min)

Table 5 S/N values of MRR and R_a

Experiment Nos.	Factors			(S/N) Ratio	
	A	B	C	MRR	R_a
1	1	1	1	−14.7747	−16.8784
2	1	2	2	−13.2949	−16.6935
3	1	3	3	−12.7015	−16.8071
4	2	1	2	−12.1355	−17.196
5	2	2	3	−10.354	−17.3352
6	2	3	1	−9.7436	−17.7197
7	3	1	3	−10.2601	−18.2306
8	3	2	1	−8.7637	−18.4794
9	3	3	2	−7.998	−18.8521

Table 6 ANOVA table for material removal rate (MRR)

Source	DF	Adj. SS	Adj. MS	F-Value	Contribution (%)
A	2	0.03229	0.016145	99.13	78.58
B	2	0.008315	0.0041575	25.52	20.24
C	2	0.00016	0.00008	0.49	0.39
Error	2	0.000326	0.000163		0.79
Total	8	0.041091			100

3 Results and Discussions

Figure 2a, b show the main effect and surface plot for Material removal rate. From Fig. 2a and Table 6 it was clear that applied voltage plays a vital role during machining followed by electrolyte concentration and wire speed (feed) for material removal rate. As the applied input voltage increases, the electrolysis process (electrochemical reaction) also increases and therefore more bubbles are formed at the tool electrode and large intensive spark is produced which is responsible to removal of a large amount of material from the quartz material. Also, higher electrolytic concentration gives a better electrolysis process and more strong bubbles are produced which is also responsible to increase the material removal rate. Wire speed plays a negligible role during the process. Figure 2b shows the surface plot of voltage and electrolyte concentration vs material removal rate. From the S/N plot, optimum parametric set for material removal rate is $A_3B_3C_3$.

Figure 3a, b show the main effect and surface plot for surface roughness. From Fig. 3a and Table 7, it is clear that applied voltage plays an important role (about 92%) during machining followed by electrolyte concentration and wire speed for surface roughness. As the applied voltage increases, the electrolysis process also increases and therefore more bubbles are formed at the tool electrode and large intensive spark is produced which is responsible for removal of a large amount of material from the quartz material. Also, a higher electrolytic concentration gives better electrolysis process and produces much stronger bubbles are produced which is responsible for increasing the material removal rate. Wire speed plays a negligible role during the process. The Electrolysis

Table 7 ANOVA table for surface roughness (R_a)

Source	DF	Adj. SS	Adj. MS	F-Value	Contribution (%)
A	2	3.60729	1.803645	67.01	92.18
B	2	0.18495	0.092475	3.44	4.73
C	2	0.06711	0.033555	1.25	1.72
Error	2	0.05383	0.026915		1.37
Total	8	3.91318			100

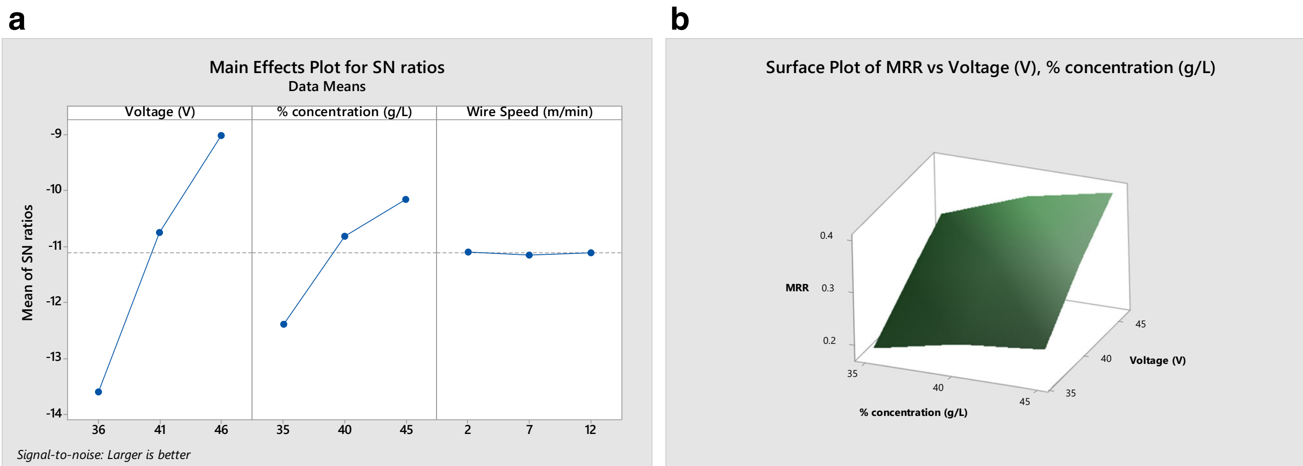

Fig. 2 **(a)** Main effect plot for MRR. **(b)** Surface plot for MRR

process increases with the applied voltage and therefore more conducting electrolyte is available for machining. Hence the gas bubble formation rate is also increased which is responsible to produce a large spark. This spark produces a rough surface on the workpiece, therefore at a higher voltage more surface roughness is found. To reduce the surface roughness, applied voltage and electrolyte concentration should be less with higher wire speed. Figure 3b shows the surface plot of voltage and electrolyte concentration vs R_a. From the S/N plot, optimum parametric set for R_a was $A_1B_1C_3$.

4 Scanning Electronic Microscope (SEM) Analysis

Figure 4a shows the SEM image of quartz glass machined with input parameters: voltage 36 V, wire speed 2 m/min and 35% electrolyte concentration (35 g/L). Figure 4a is the result of continuous machining for 25 min with 0.15-mm-diameter Zn layered brass wire. At lower levels of input parameters, the low energy available at the tool-electrolyte interface, governed by Eq. 1. There is low rate of bubble formation, as the electrochemical reaction rate is low at lower levels. This leads to smooth and controlled machining of the workpiece. However, small debris has been observed at machined surface. This might be due to improper melting and vaporization of the workpiece.

Figure 4b shows the SEM image of material machined at input parameters: voltage 46 V, wire speed 7 m/min, and 45% electrolyte concentration (45 g/L). For higher levels of input parameters, the rate of bubble formation is high as the electrochemical reaction rate is high which leads to sparking. The intensity of sparking is so high that it leaves the micro-cracks and uneven surface which appears as contour edges. Edge necking is observed at the beginning of micro-slot, which might be due to stray erosion as quartz glass offers initial resistance because of fractural toughness.

Furthermore, it has been observed that the length of cut (LOC) is increased with voltage and electrolyte concentration.

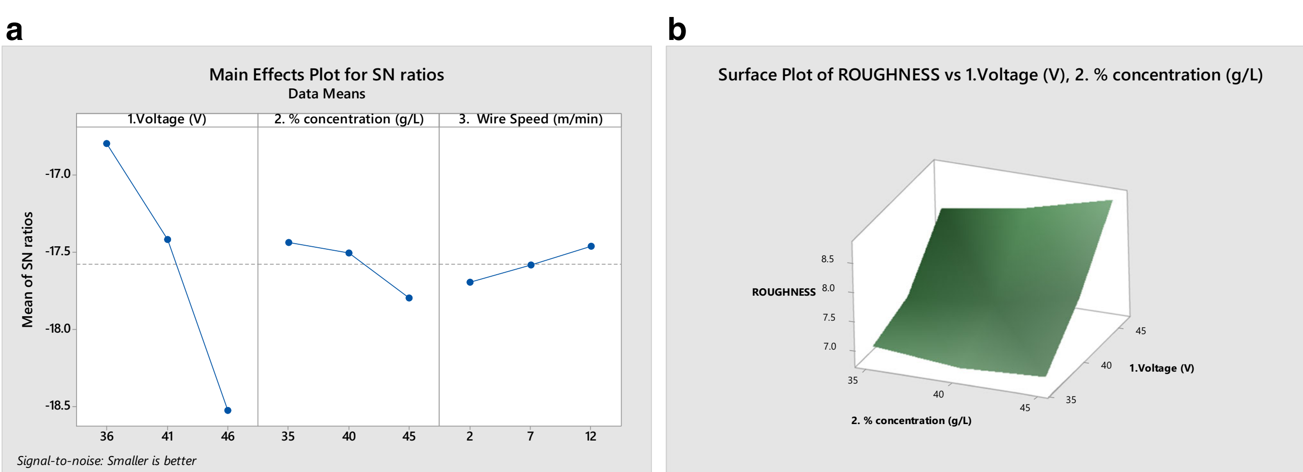

Fig. 3 **(a)** Main effect plot for $SR(R_a)$. **(b)** Surface plot for $SR(R_a)$

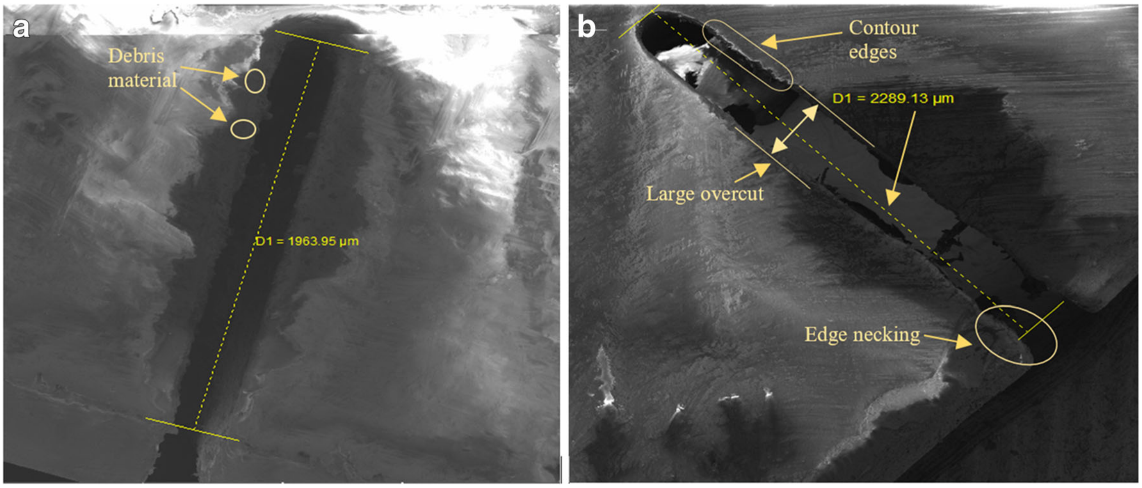

Fig. 4 SEM image for experimental condition **(a)** Voltage 36 V, Electrolyte concentration 35% (g/L) and wire speed 2 m/min **(b)** SEM image for experimental condition Voltage 46 V, Electrolyte concentration 45% (g/L) and wire speed 7 m/min

5 Mathematical Models

The multiple regression model was used to derive the relationship among the governing input parameters to response characteristics by fitting the linear equation for experimentally observed values. The interaction of input parameters is not considered due to selected L_9 orthogonal array. However, the fixed parameters such as tool wire, workpiece, auxiliary electrode, electrolyte were considered as the constraint while developing the mathematical model. The following mathematical equations can be used for machining the quartz glass using wire electrochemical discharge machining process at different operating conditions keeping the other constant parameters in knowledge. Eq. 4 and 5 show the mathematical model for MRR and R_a respectively.

A mathematical model for material removal rate (mg/min) is

$$MRR = -0.5985 + 0.01464 \times V + 0.00730 \times E - 0.00102 \times W_S \quad R^2\ (\mathrm{MRR}) = 98\% \tag{4}$$

A mathematical model for surface roughness (micrometer) is

$$R_a = 0.1588 + 0.1525 \times V + 0.0333 \times E - 0.0209 \times W_s \quad R^2\ (\mathrm{Ra}) = 95\% \tag{5}$$

Where V is the voltage (Volt), E is the electrolyte concentration (g/l), W_s is the wire speed (m/min) and R^2 is the coefficient of determination.

6 Additivity Test

It is necessary to validate the developed mathematical model whether it holds good for an intermediate combination of input parameters other than an orthogonal array. Therefore, experiments are performed to confirm its validity. Table 8 represents the combination of input parameters and response values obtained experimentally. The percentage error shows the deviation of experimental values from predicted mathematical values. From Table 8, it is evident that the error percentage always less than 6%. The results show the developed mathematical model is valid with experimental values.

7 Conclusions

In the present study, zinc-layered brass wire is utilized during the machining of hard and brittle quartz material. An experimental investigation is carried out to study the influence of input process parameters. The following conclusions are

Table 8 Additivity test

WECDM Parameters			Material removal rate (MRR)			Surface roughness (SR)		
A	B	C	Experimental Values	Predicted Value based on Mathematical equation	Error (%)	Experimental Values	Predicted Value based on Mathematical equation	Error (%)
39	38	4	0.24071	0.24578	2.06	6.9272	7.2881	4.95
43	41	8	0.32157	0.32216	0.18	7.4523	7.9144	5.83
45	44	11	0.36082	0.37028	2.55	7.9561	8.2566	3.79

drawn after the experimental study on the material removal rate and surface roughness characteristics for micro-machining of quartz material.

1) An in-house WECDM setup can successfully machine the non-conducting quartz material with considerable accuracy and precision.
2) Layered wire provides better machining characteristics in terms of surface roughness and material removal rate. Also, it improves the machining performance by reducing the wire breakage.
3) SEM images show the regular and smooth surface obtained at the lower levels of input parameters compared to higher-end levels. At a higher level, shallow cracks with slight necking at the beginning of the machined surface and higher length cuts are observed.
4) Based on a signal to noise (S/N) ratio, higher voltage and electrolyte concentration are suggested for higher material removal rate as ANOVA result reveals that they contribute 78.58% and 20.23% respectively.
5) For a lower surface finish, voltage and electrolyte concentration are the most significant factors. An ANOVA result reveals that voltage and electrolyte concentration contributions are 92.18% and 4.72% respectively.
6) The developed mathematical model is in agreement with experimental results, therefore, it has immense potential to calculate the surface roughness and material removal rate under different parametric combinations.
7) It is also observed that during machining of quartz, debris gets embedded at the workpiece and in the wire gap (machining gap). This might be due to the improper flushing across the machined surface. This can be improved by deploying the flushing pump with a suitable discharge.

References

1. Singh J, Vaishya R, Kumar M (2019) Fabrication of microfeatures on quartz glass using developed WECDM setup. ARPN J Eng Appl Sci 14:725–731
2. Puttick KE, Rudman MR, Smith KJ, Franks A, Lindsey K (1989) Single-point diamond machining of glasses. Proc R Soc Lond A 426:19–30. https://doi.org/10.1098/rspa.1989.0116
3. Guzzo PL, Raslan AA, De Mello JDB (1999) Relationship between quartz crystal orientation and the surface quality obtained by ultrasonic machining, in joint meeting. Micropolis 792–795. https://doi.org/10.1109/FREQ.1999.841424
4. Fabian S, Hlaváˇ LM, Hlaváˇ IM et al (2009) Experimental method for the investigation of the abrasive water jet cutting quality. J Mater Process Technol 209:6190–6195. https://doi.org/10.1016/j.jmatprotec.2009.04.011
5. Hildebrand J, Hecht K, Bliedtner J, Müller H (2011) Laser beam polishing of quartz glass surfaces. Phys Procedia 12:452–461. https://doi.org/10.1016/j.phpro.2011.03.056
6. Jain VK, Rao PS, Choudhary SK, Rajurkar KP (2016) Experimental investigations into Traveling Wire Electrochemical Spark Machining (TW-ECSM) of composites. J Eng Ind 113:75–84. https://doi.org/10.1115/1.2899625
7. Oza AD, Kumar A, Badheka V, Arora A (2019) Traveling Wire Electrochemical Discharge Machining (TW-ECDM) of quartz using zinc coated Brass wire: investigations on material removal rate and kerf width characteristics. Silicon. https://doi.org/10.1007/s12633-019-0070-y
8. Yang CT, Song SL, Yan BH, Huang FY (2006) Improving machining performance of wire electrochemical discharge machining by adding SiC abrasive to electrolyte. Int J Mach Tools Manuf 46:2044–2050. https://doi.org/10.1016/j.ijmachtools.2006.01.006
9. Kuo KY, Wu KL, Yang CK (2015) Effect of adding SiC powder on surface quality of quartz glass microslit machined by WECDM. Int J Adv Manuf Technol 78:73–83. https://doi.org/10.1007/s00170-014-6602-0
10. Bhuyan BK, Yadava V (2014) Modelling and optimisation of travelling wire electro-chemical spark machining process. Int J Ind Syst Eng 18:139–158. https://doi.org/10.1504/IJISE.2014.064703
11. Rattan N, Mulik RS (2017) Experimental investigations and multi-response optimization of silicon dioxide (quartz) machining in magnetic field assisted TW-ECSM process. Silicon 9:663–673. https://doi.org/10.1007/s12633-016-9521-x
12. Rattan N, Mulik RS (2017) Improvement in material removal rate (MRR) using magnetic field in TW-ECSM process. Mater Manuf Process 32:101–107. https://doi.org/10.1080/10426914.2016.1176197
13. Bhuyan BK, Yadava V (2014) Experimental study of traveling wire electrochemical spark machining of borosilicate glass. Mater Manuf Process 29:298–304. https://doi.org/10.1080/10426914.2013.852216
14. Bhuyan BK, Yadava V (2014) Experimental modelling and multi-response optimization of travelling wire electrochemical spark machining of Pyrex glass. Proc Inst Mech Eng Part B J Eng Manuf 228:902–916. https://doi.org/10.1177/0954405413514745
15. Peng WY, Liao YS (2004) Study of electrochemical discharge machining technology for slicing non-conductive brittle materials. J Mater Process Technol 149:363–369. https://doi.org/10.1016/j.jmatprotec.2003.11.054
16. Mitra NS, Doloi B, Bhattacharyya B (2015) Predictive analysis of criterial yield during travelling wire electrochemical discharge machining of Hylam based composites. Adv Prod Eng Manag 10:73–86. https://doi.org/10.14743/apem2015.2.193
17. Malik A, Manna A (2016) An experimental investigation on developed WECSM during micro slicing of e-glass fibre epoxy composite. Int J Adv Manuf Technol. https://doi.org/10.1007/s00170-016-8858-z
18. Liu JW, Yue TM, Guo ZN (2009) Wire electrochemical discharge machining of Al2O3 particle reinforced aluminum alloy 6061. Mater Manuf Process 24:446–453. https://doi.org/10.1080/10426910802714365
19. Yadav P, Yadava V, Narayan A (2018) Experimental investigation of kerf characteristics through wire electrochemical spark cutting of alumina epoxy nanocomposite. J Mech Sci Technol 32:345–350. https://doi.org/10.1007/s12206-017-1234-6
20. Kuo KY, Wu KL, Yang CK, Yan BH (2013) Wire electrochemical discharge machining (WECDM) of quartz glass with titrated electrolyte flow. Int J Mach Tools Manuf 72:50–57. https://doi.org/10.1016/j.ijmachtools.2013.06.003
21. Basak I, Ghosh A (1996) Mechanism of spark generation during electrochemical discharge machining: a theoretical model and experimental verification. J Mater Process Technol 62:46–53. https://doi.org/10.1016/0924-0136(95)02202-3
22. Basak I, Ghosh A (1997) Mechanism of material removal in electrochemical discharge machining: a theoretical model and

experimental verification. J Mater Process Technol 71:350–359. https://doi.org/10.1016/S0924-0136(97)00097-6
23. Crichton IM, McGeough JA (1985) Studies of the discharge mechanisms in electrochemical arc machining. J Appl Electrochem 15: 113–119. https://doi.org/10.1007/BF00617748
24. Jain VK, Dixit PM, Pandey PM (1999) On the analysis of the electrochemical spark machining process. Int J Mach Tools Manuf 39:165–186. https://doi.org/10.1016/S0890-6955(98)00010-8